Nonclassical effects of a driven atoms-cavity system in the presence of an arbitrary driving field and dephasing

J. P. Clemens and P. R. Rice
Department of Physics, Miami University, Oxford, Ohio 45056
(Received 23 July 1999; revised manuscript received 18 January 2000; published 15 May 2000)

We investigate the photon statistics of light transmitted from a driven optical cavity containing one or two atoms interacting with a single mode of the cavity field. We treat arbitrary driving fields with emphasis on departure from previous weak field results. In addition effects of dephasing due to atomic transit through the cavity mode are included using two different models. We find that both models show the nonclassical correlations are quite sensitive to dephasing. The effect of multiple atoms on the system dynamics is investigated by placing two atoms in the cavity mode at different positions, therefore having different coupling strengths.

PACS number(s): 42.50.Ct, 42.50.Lc, 42.50.Ar

I. INTRODUCTION

In this paper we report on extensions to previous work on dynamical cavity QED effects in the photon statistics of transmitted light from a driven optical cavity coupled to an ensemble of two-level atoms. Much work has been done on structural cavity QED effects such as energy level shifts and the modification of spontaneous emission rates. These structural effects can be seen to arise from semiclassical models. In addition, work has been done on dynamical effects where the coupling between the cavity field and atoms has a significant effect on the evolution of the system, in particular in the strong coupling regime where a single quantum of energy and hence single quantum fluctuations give rise to nontrivial dynamics. In this regime the field cannot be viewed as mildly perturbed by the atoms (good cavity limit), nor are the atoms mildly perturbed by the field (bad cavity limit). For a review of the work on structural and dynamical effects in cavity QED, see Ref. [1].

The problem of a single two-level atom coupled to a single-mode field was originally studied by Jaynes and Cummings [2] and extended to many atoms by Tavis and Cummings [3,4]. These models have been extended in recent theoretical work to include spontaneous emission and cavity field decay [5,6], and atomic transit time broadening and detunings [7]. Nonclassical correlations in photon statistics that violate a Schwarz inequality have been predicted for this system, including photon antibunching [defined here as $g^{(2)}(0)_{+}>g^{(2)}(0)$], and sub-Poissonian statistics [$g^{(2)}(0)<1$]. Other effects have also been predicted, which we refer to as overshoots and undershoots [$|g^{(2)}(\tau)-1|>|g^{(2)}(0)-1|$, where $g^{(2)}(\tau)$ is the normalized second-order correlation function]. Examples of these nonclassical correlations from previous weak field results are shown in Fig. 1. Figure 1(a) shows photon antibunching and sub-Poissonian statistics, (b) shows an overshoot violation, and (c) shows an undershoot violation.

Photon antibunching has been seen experimentally in this system by Rempe *et al.* [8]. Overshoot violations have recently been seen by Mielke, Foster, and Orozco [9]. In general, the theory matches the experiments in terms of qualitative behavior while the quantitative size of the nonclassical effect does not. This has led us to consider complications in the experiments that may be responsible for the discrepancy, including deviations from the weak field limit and dephasing due to the atoms entering and leaving the cavity. The experiments use an atomic beam to introduce atoms into the cavity so that the time of flight across the mode is on the order of ten spontaneous emission lifetimes [9]. We expect that dephasing due to atomic traversal of the cavity will have a detrimental effect on nonclassical correlations. In addition, deviations from the weak driving field limit and interactions with ''spectator'' atoms far from the mode waist may be important. These effects are investigated in this paper by numerically solving the master equation for the system and

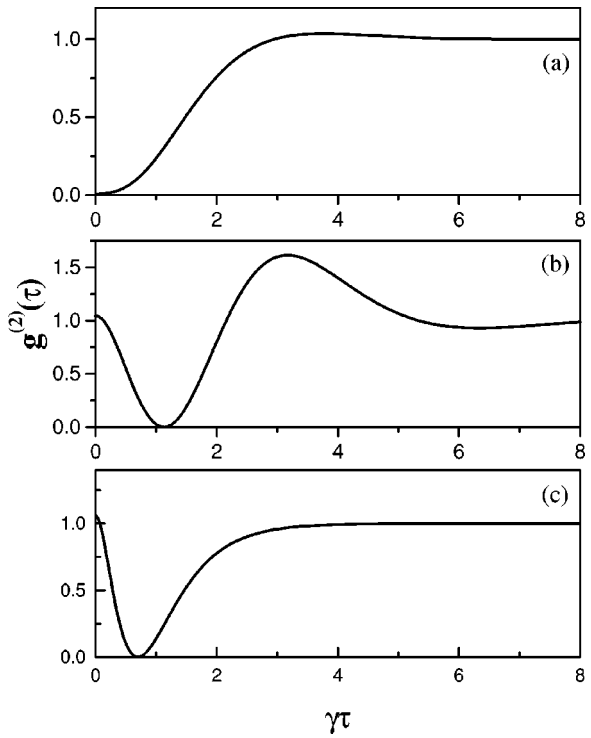

FIG. 1. Examples of nonclassical photon statistics in the weak field limit. (a) Sub-Poissonian statistics and photon antibunching; (b) an overshoot violation of the Schwarz inequality; (c) an undershoot violation of the Schwarz inequality.

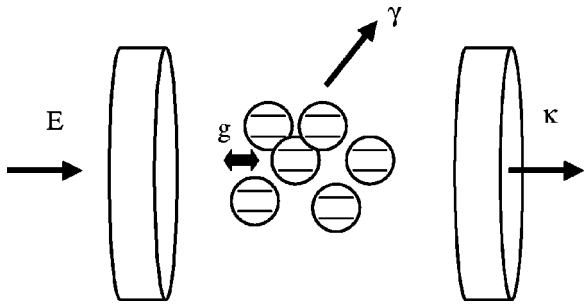

FIG. 2. A diagram of the system. The cavity field decays at a rate κ, the atom spontaneously emits at a rate γ, and there is an electric dipole coupling between the atom and cavity field with a strength g.

by quantum trajectory simulations. Rather than investigating all possible effects at once, we isolate them and try to understand what is most critical.

The general outline of this paper is as follows. In Sec. II we present the physical model of the system under investigation and describe the methods of solution. In Sec. III we discuss the photon statistics of the transmitted light outside the weak field limit. Section IV presents two models of atomic transit dephasing and the resulting photon statistics. In Sec. V we include effects of a spectator atom with a coupling that is a fraction of the maximum coupling, and finally we conclude in Sec. VI.

II. PHYSICAL MODEL

The system under investigation is an extension of the Jaynes-Cummings Hamiltonian to include effects of atomic and cavity field decay as well as a coherent driving field. A schematic diagram of the system is shown in Fig. 2. The field and atomic Hamiltonians are given by

$$H_F=\hbar\omega_c a^\dagger a, \tag{1}$$

$$H_A=\sum_j \hbar\omega_a\sigma_z^j, \tag{2}$$

and the atom-field interaction in the rotating wave approximation is given by

$$H_{AF}=\sum_j i\hbar g_j(a^\dagger\sigma_-^j-a\sigma_+^j). \tag{3}$$

The cavity field creation and annihilation operators are $a^\dagger$ and a, respectively, and $\sigma_\pm^j$ and σ_z^j are Pauli operators for the jth two-level atom. The atom-field coupling strength is determined by

$$g_j=\mu\left(\frac{\omega_c}{2\hbar\epsilon_0 V}\right)^{1/2}\sin kz_j, \tag{4}$$

where μ is the dipole transition matrix element between the two atomic states, V is the cavity mode volume, and $\sin kz_j$ takes into account the position of the atom in the mode. In previous work it was assumed that the atoms are at antinodes of the field where the coupling is a maximum. In this paper we allow the atoms to be placed anywhere in the mode so that a range of couplings is allowed for different atoms. The cavity field is driven by a classical laser field with the driving field–cavity field coupling described by the Hamiltonian

$$H_L=i\hbar E(a^\dagger e^{-i\omega_d t}-ae^{i\omega_d t}), \tag{5}$$

where E is the classical laser intensity scaled such that E/κ is the photon flux injected into the cavity. Throughout the paper we assume the atom, cavity field, and driving field are on resonance ($\omega_0\equiv\omega_c=\omega_a=\omega_d$).

Dissipation in the system gives rise to nontrivial irreversible dynamics. Cavity field damping and atomic population and polarization decay are described by superoperators acting on the density matrix of the system which are derived using standard methods [10,11]. Cavity field damping is described by

$$\mathcal{L}_F\rho=\kappa(2a\rho a^\dagger-a^\dagger a\rho-\rho a^\dagger a), \tag{6}$$

where κ is the rate of cavity field damping. Atomic population and polarization decay are described by

$$\mathcal{L}_A\rho=\frac{\gamma}{2}\sum_j(2\sigma_-^j\rho\sigma_+^j-\sigma_+^j\sigma_-^j\rho-\rho\sigma_+^j\sigma_-^j), \tag{7}$$

where γ is the spontaneous emission rate of an atom. The full master equation in the Born-Markov approximation is then

$$\dot\rho=-\frac{i}{\hbar}[H_A+H_F+H_{AF}+H_L,\rho]+\mathcal{L}_F\rho+\mathcal{L}_A\rho\rightarrow\mathcal{L}\rho. \tag{8}$$

A numerical solution of the master equation is carried out in the Fock state basis, and also a quantum trajectory simulation is developed from the master equation.

A. Numerical solution of the master equation

The master equation in the Fock state basis is

$$\begin{aligned}\dot\rho_{n,+;m,+}=&-g\sqrt{n+1}\rho_{n+1,-;m,+}-g\sqrt{m+1}\rho_{n,+;m+1,-}\\&+E\sqrt{n}\rho_{n-1,+;m,+}+E\sqrt{m}\rho_{n,+;m-1,+}\\&-E\sqrt{n+1}\rho_{n+1,+;m,+}-E\sqrt{m+1}\rho_{n,+;m+1,+}\\&+2\kappa\sqrt{(n+1)(m+1)}\rho_{n+1,+;m+1,+}\\&-[\kappa(n+m)+\gamma]\rho_{n,+;m,+},\end{aligned} \tag{9a}$$

$$\begin{aligned}\dot\rho_{n,-;m,-}=&\,g\sqrt{n}\rho_{n-1,+;m,-}+g\sqrt{m}\rho_{n,-;m-1,+}\\&+E\sqrt{n}\rho_{n-1,-;m,-}+E\sqrt{m}\rho_{n,-;m-1,-}\\&-E\sqrt{n+1}\rho_{n+1,-;m,-}-E\sqrt{m+1}\rho_{n,-;m+1,-}\\&+2\kappa\sqrt{(n+1)(m+1)}\rho_{n+1,-;m+1,-}\\&-\kappa(n+m)\rho_{n,-;m,-}+\gamma\rho_{n,+;m,+},\end{aligned} \tag{9b}$$

$$\dot{\rho}_{n,+;m,-} = -g\sqrt{n+1}\rho_{n+1,+;m,-} + g\sqrt{m}\rho_{n,+;m-1,+} + E\sqrt{n}\rho_{n-1,+;m,-} + E\sqrt{m}\rho_{n,+;m-1,-} - E\sqrt{n+1}\rho_{n+1,+;m,-} - E\sqrt{m+1}\rho_{n,+;m+1,-} + 2\kappa\sqrt{(n+1)(m+1)}\rho_{n+1,+;m+1,-} - [\kappa(n+m) - \gamma/2]\rho_{n,+;m,-}, \tag{9c}$$

$$\dot{\rho}_{n,-;m,+} = \dot{\rho}^*_{m,+;n,-}, \tag{9d}$$

where $\rho_{n,\pm;m,\pm} = \langle n,\pm|\rho|m,\pm\rangle$ and + and − denote upper and lower atomic states, respectively.

We have numerically solved the master equation for the steady state for arbitrary driving field by truncating the Fock basis at a point where the population of $|n_{max},\pm\rangle$ is less than 10^{-4}. The second-order correlation function

$$g^{(2)}(\tau) = \frac{\langle a^\dagger(0)a^\dagger(\tau)a(\tau)a(0)\rangle}{\langle a^\dagger a\rangle^2_{ss}} \tag{10}$$

is calculated from steady state matrix elements using the quantum regression theorem due to Lax [12]. This correlation function is, of course, the conditional probability of detecting a photon at $t=\tau$, conditioned on detecting one at $t=0.0$. It is normalized to the conditional probability one obtains from a field in a coherent state.

B. Quantum trajectory simulation

We have developed a quantum trajectory simulation of this system from the master equation following the formalism of Carmichael [13]. We unravel the master equation into a piece describing continuous evolution and a set of collapse operators in a way that is based on a simulated photon counting experiment,

$$\mathcal{L}\rho = (\mathcal{L}-S)\rho + \mathcal{S}\rho, \tag{11}$$

where $(\mathcal{L}-S)\rho$ is identified as the terms that can be written as commutators or anticommutators and $\mathcal{S}\rho$ is identified as all terms which can be written as $\hat{O}^\dagger\rho\hat{O}$. This particular unraveling is well suited for studies of photon statistics as the $\hat{O}$'s represent quantum jumps due to emission of a photon. The continuous evolution of the system is described by $(\mathcal{L}-\mathcal{S})\rho$ while $\mathcal{S}\rho$ describes collapse events which punctuate the evolution. We define a closed system Hamiltonian and a dissipative Hamiltonian from the unraveled master equation as

$$(\mathcal{L}-\mathcal{S})\rho = -\frac{i}{\hbar}[H_S,\rho] + [H_D,\rho]_+ = -\frac{i}{\hbar}[H_A + H_F + H_{AF} + H_L,\rho] - \left[\left(a^\dagger a + \sum_j \sigma^j_+\sigma^j_-\right),\rho\right]_+, \tag{12}$$

where $[\hat{O},\rho]_+$ denotes the anticommutator of $\hat{O}$ and ρ. A non-Hermitian Hamiltonian that reproduces the continuous evolution of the density matrix is defined as

$$H = H_S + i\hbar H_D. \tag{13}$$

The rest of the master equation enters as collapse operators which are applied at random times when $R(0,1) < P_c$, where $R(0,1)$ is a random number between zero and 1 and

$$P_c = \langle\psi|\hat{O}^\dagger\hat{O}|\psi\rangle\, dt. \tag{14}$$

In our system we have two collapse operators, corresponding to spontaneous emission out of the side of the cavity and photons lost through the cavity mirror,

$$O_{spon.em.} = \sqrt{\gamma}\sigma_-, \tag{15a}$$

$$O_{cavityloss} = \sqrt{2\kappa}a. \tag{15b}$$

The time step size is $(20r)^{-1}$ where r is the fastest rate in the problem. In the event that both collapse probabilities (for spontaneous emission and cavity emission) are greater than the random number, yielding two collapse processes in a single time step, we use a random number to choose one of the collapses. The time step is small enough that very few of these events happen, if any. At each time step, the wave function must be normalized. If the random number is such that we perform Hamiltonian evolution, the norm is not preserved as the trajectory Hamiltonian is non-Hermitian. Also, a collapse operator must be augmented by normalization, as the norm changes upon application of the collapse operator. In Sec. IV we describe dephasing due to an atom leaving the cavity using another collapse operator.

Because this unraveling of the master equation is based on photon counting experiments, the calculation of the second-order correlation function is carried out quite naturally. The collapse operator $\hat{a}$ corresponds to emission and detection of a photon from the cavity field mode. We calculate $g^{(2)}(\tau)$ by building up a histogram of delay times between photon detections averaged over a long evolution time in a way analogous to experimental measurement.

The photon statistics of the transmitted light have already been calculated in the weak field limit using a truncated five-state basis where the system has up to two quanta of energy in it [5]. The three types of nonclassical behavior previously discussed have been seen in subsequent experiments; however, current experiments are not strictly in the weak field limit. It is of interest then to calculate the photon statistics for arbitrary driving field and to see to what extent the nonclassical effects persist. It is expected that for strong enough driving field, the atoms will saturate and the nonclassical photon correlations will be washed out as the cavity will essentially contain a coherent state that is only mildly perturbed by the presence of the atom.

Let us look at the photon correlations in the weak field limit from the point of view of quantum trajectories. In this case the system can be described in the steady state by a wave function, as described in [6]. The detection of the first photon emitted from the steady state collapses the wave

function of the system ($|\psi_{ss}\rangle \rightarrow a|\psi_{ss}\rangle$) and the subsequent time evolution as the system returns to the steady state determines the photon correlations. The second-order correlation function is given by the probability of detecting a second photon normalized to the probability of detecting a photon in the steady state,

$$g^{(2)}(\tau) = \frac{\langle a^\dagger(\tau) a(\tau)\rangle_c}{\langle a^\dagger a\rangle_{ss}}. \tag{16}$$

From a trajectory point of view we can interpret Eq. (16) as the relative probability of a second cavity decay coming at time τ, given that one occurred at $t=0.0$. This is because the cavity collapse event probability is proportional to the mean photon number. This is extremely small in the weak field limit, and so the most common thing after an emission of a photon out of the cavity is that the system evolves back to the steady state. Only very occasionally for very weak fields does a second collapse occur before the system returns to steady state. Also, spontaneous emission events, where the atom emits out of the side of the cavity, are proportional to the excited state probability, which again is small for weak fields. So rarely do we get a cavity or spontaneous emission collapse, and thus even more rarely two collapses in a time span on the order of κ^{-1} or γ^{-1}. Experimentally, these event pairs are the source of delayed coincidence counts. For weak fields, the rarity of these events means long counting times. In the trajectory formalism, this is also the case, except that we can ignore the long times the atom spends in the steady state before the next collapse. In the weak field limit, for the trajectory calculations, we start the system in the steady state, collapse the wave function, and let it evolve to get $g^{(2)}(\tau)$, as in [7].

An example of this is shown in Fig. 3 for the case of the overshoot violation, where the above formula reproduces the earlier results [5,6]. Outside the weak field limit the photon correlations are altered for two reasons. Most simply, the time evolution following a collapse from steady state will be altered by the stronger driving field. Another effect, however, is the presence of multiple collapses before the system returns to the steady state. Consider a multiple-collapse process. The first photon comes from the steady state and collapses the wave function of the system ($|\psi_{collapse1}\rangle = a|\psi_{ss}\rangle$). Now the time evolution occurs as before. However, the second photon collapses the system to a new state which depends on the delay time since the emission of the first photon [$|\psi_{collapse2}\rangle = a|\psi_{collapse1}(\tau)\rangle$]. If a third photon is emitted before the system returns to steady state then its delay time will depend on the details of the evolution from $|\psi_{collapse2}\rangle$. When averaged over many instances, this process will wash out the nonclassical effects because of the different evolution following different $|\psi_{collapse2}\rangle$. To obtain $g^{(2)}(\tau)$, outside the weak field limit, we start the system in the ground state, and let it evolve for 10–20 cavity or atomic lifetimes (whichever is longest), and then keep track of the time between cavity emission events and build up a histogram of photon detection delay times. This is exactly what is done experimentally. After a cavity emission event, we record the time till the next 10 or so cavity emissions. This histogram is turned into $g^{(2)}(\tau)$ by normalizing the long delay time value to unity.

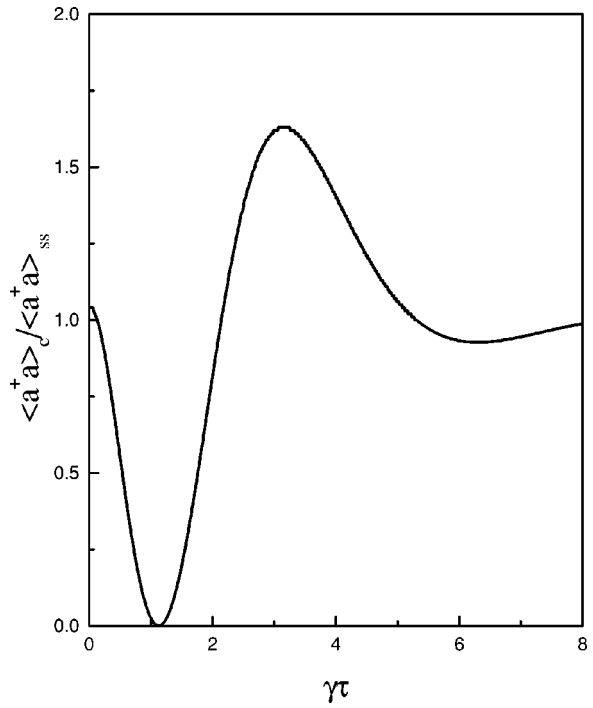

FIG. 3. The conditioned photon number normalized by the steady state photon number for the cavity field. This is identical to $g^{(2)}(\tau)$ in the weak field limit. Parameters are $g/\gamma=1$, $\kappa/\gamma=0.77$, and $E/\gamma=0.01$.

III. NONWEAK DRIVING FIELD

To obtain results outside the weak field limit, we pursue the density matrix approach. The computations are much faster than the trajectory method. $N(N-1)/2$ equations (with N the total number of states) are solved instead of N, but in the trajectory approach those N equations must be solved many times, usually averaging over a million or so realizations. The trajectories can still help us untangle the physics involved, however. Figure 4 shows the time evolution of $\langle a^\dagger a\rangle_c$ following a photon emission from the steady state for a variety of system parameters. The overshoot persists in the evolution of the field following emission of a photon from the cavity for a driving field as large as $E/E_{sat}=0.41$. The undershoot and sub-Poissonian statistics survive for driving fields as large as $E/E_{sat}=0.8$ and $E/E_{sat}=0.37$, respectively. The saturation field strength E_{sat} is the driving field for which

$$\langle n\rangle = n_{sat} = \frac{\gamma^2}{8g^2}. \tag{17}$$

The photon statistics of the transmitted field are shown in Fig. 5 for the three types of nonclassical effects seen in this system at a variety of driving field intensities. Figure 5(a) shows $g^{(2)}(\tau)$ for system parameters ($g/\gamma=1, \kappa/\gamma=0.77$)

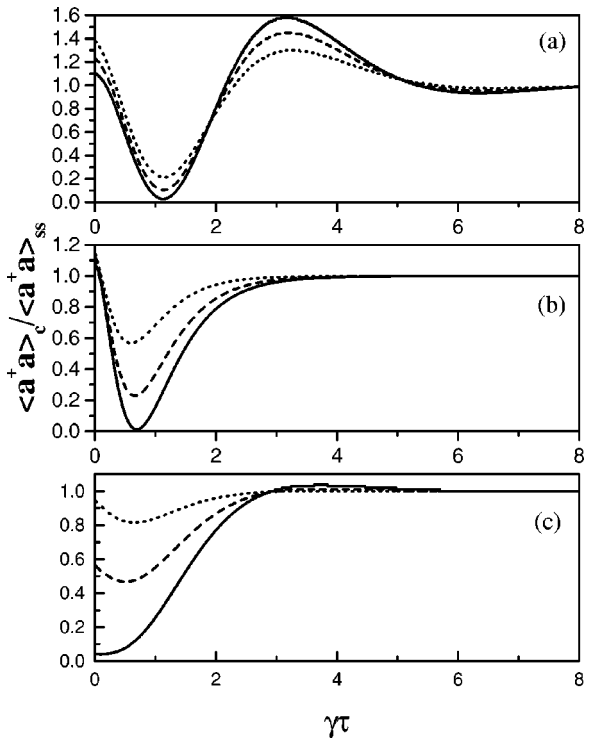

FIG. 4. Time evolution of the conditioned cavity photon number following emission of a photon from the cavity and collapse of the wave function from steady state. The plots are for (a) $g/\gamma=1$, $\kappa/\gamma=0.77$, $E/\gamma=0.1$ (solid line), 0.2 (dashed line), 0.3 (dotted line); (b) $g/\gamma=2$, $\kappa/\gamma=5$, $E/\gamma=0.1$ (solid line), 0.5 (dashed line), 1 (dotted line); (c) $g/\gamma=1$, $\kappa/\gamma=1.6$, $E/\gamma=0.1$ (solid line), 0.5 (dashed line), 1 (dotted line).

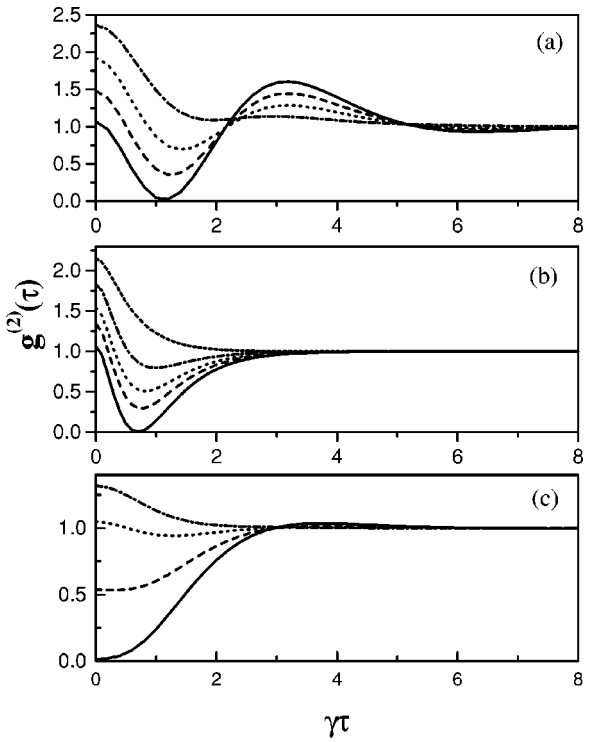

FIG. 5. Photon statistics of the transmitted field for varying driving field strength. The plots are for (a) $g/\gamma=1$, $\kappa/\gamma=0.77$, $E/\gamma=0.025$ (solid line), 0.125 (dashed line), 0.2 (dotted line), 0.35 (dash-dotted line); (b) $g/\gamma=2$, $\kappa/\gamma=5$, $E/\gamma=0.025$ (solid line), 0.25 (dashed line), 0.35 (dotted line), 0.5 (dash-dotted line), 1 (small-dashed line); (c) $g/\gamma=1$, $\kappa/\gamma=1.6$, $E/\gamma=0.025$ (solid line), 0.25 (dashed line), 0.425 (dotted line), 0.6 (dash-dotted line).

that produce an overshoot violation of the Schwarz inequality $[g^{(2)}(\tau)>g^{(2)}(0)]$ in the weak field limit. At a driving field of $E/E_{sat}=0.17$ the overshoot violation is gone; thus this nonclassical effect is quite dependent on the weak driving field. Figure 5(b) shows photon statistics for system parameters $(g=2/\gamma,\kappa/\gamma=5)$ that produce an undershoot violation of the Schwarz inequality $[1-g^{(2)}(\tau)_{min}>g^{(2)}(0)-1]$ in the weak field limit. Here the nonclassical effect disappears at a driving field of $E/E_{sat}=0.28$, showing that this is a more robust effect. Figure 5(c) shows photon statistics for system parameters $(g/\gamma=1,\kappa/\gamma=1.6)$ that produce photon antibunching $[g^{(2)}(0)_+>g^{(2)}(0)]$ and sub-Poissonian statistics $[g^{(2)}(0)<1]$ in the weak field limit. In this case the nonclassical effect persists until $E/E_{sat}=0.16$ where the system shows slight bunching and super-Poissonian statistics. (Notice that the nonclassical effects are not as robust as the time evolution of the cavity field would indicate. Therefore the destruction of nonclassical effects is in part a result of multiple-photon processes.) For all system parameters the transmitted light becomes super-Poissonian as the driving field is increased.

IV. ATOMIC TRANSIT DEPHASING

We now turn our attention to the effects of atomic traversal of the cavity on the photon statistics. In previous work it has been assumed that the atoms are all fixed at antinodes of the cavity field and so have the maximum coupling $g_0=\mu(\omega_c/2\hbar\epsilon_0 V)^{1/2}$. Experiments on this system have used atomic beams to send atoms through a cavity. This atomic traversal of the cavity will introduce two new effects. First, the atom-cavity field coupling will depend on the position of the atom in the cavity, which changes in time as the atom traverses the cavity. One might think that this would destroy the nonclassical correlations. However, the atoms with the largest coupling interact most strongly with the field and are most likely to contribute to the correlations. So the atoms near an antinode will have the largest contribution and other atoms may have little effect on the correlations. This issue will be further addressed in Sec. V. The second effect of atomic traversal is dephasing, which occurs when an atom enters or leaves the cavity. It is this effect that we consider in this section.

We have used two approaches to model the dephasing due to atomic traversal. The first, and most common for theorists to use, is to add a term to the master equation which describes nonradiative decay of atomic polarization

$$\dot{\rho}=\mathcal{L}\rho+\gamma_{ph}(\sigma_z\rho\sigma_z-\rho). \tag{18}$$

This term in the master equation has its origins in collisional processes [11] and so may or may not accurately describe the

dephasing that occurs when an atom leaves the cavity. For this approach, we use density matrix methods and the quantum regression theorem to calculate $g^{(2)}(\tau)$. We refer to this as *collisional* dephasing.

The second approach uses a quantum trajectory simulation of the system to model the dephasing. In this approach we assume that there is always exactly one atom in the cavity. An atom leaves the cavity and another atom enters the cavity in the ground state at a rate γ_{ph}. The atom enters the cavity in the ground state, but it is not immediately clear how to deal with the atom that leaves the cavity. This atom is in some superposition of excited and ground states and these states are entangled with the cavity field state. One approach would be to leave the photon number distribution of the cavity field unchanged using a collapse operator, which has the following action on the state of the system:

$$|\psi\rangle = \sum_n \left(c_{e,n}|e,n\rangle + c_{g,n}|g,n\rangle\right) \rightarrow |\psi_c\rangle$$

$$= \sum_n \left(c_{e,n}^2 + c_{g,n}^2\right)|g,n\rangle. \tag{19}$$

However, this is not a consistent application of the quantum trajectories. Consider the evolution of the atom after it leaves the cavity. The atom at some later time may emit a photon into the vacuum, meaning it was in the excited state when it left the cavity. Or it will never emit a photon, meaning it was in the ground state when it left the cavity. In general, the atom and environment and by entanglement the atom-cavity system will then be described by a density operator. However, we wish to use a pure state to describe the atom-cavity system conditioned on the detection of transmitted photons. To be consistent we must use a pure state to describe the atom after it has left the cavity. This corresponds to following the atom after it has left the cavity and determining whether it ever emits a photon or not. Rather than actually follow the atom in the calculation, we use a collapse operator that picks either the excited state field distribution or the ground state field distribution of the system and then places the new atom in the ground state. This operator has the following action:

$$|\psi\rangle = \sum_n \left(c_{e,n}|e,n\rangle + c_{g,n}|g,n\rangle\right) \rightarrow |\psi_c\rangle$$

$$= \sum_n c_{e,n}|g,n\rangle \quad \text{with probability} \quad \sum_n c_{e,n}^2, \tag{20a}$$

$$|\psi\rangle = \sum_n \left(c_{e,n}|e,n\rangle + c_{g,n}|g,n\rangle\right) \rightarrow |\psi_c\rangle$$

$$= \sum_n c_{g,n}|g,n\rangle \quad \text{with probability} \quad \sum_n c_{g,n}^2. \tag{20b}$$

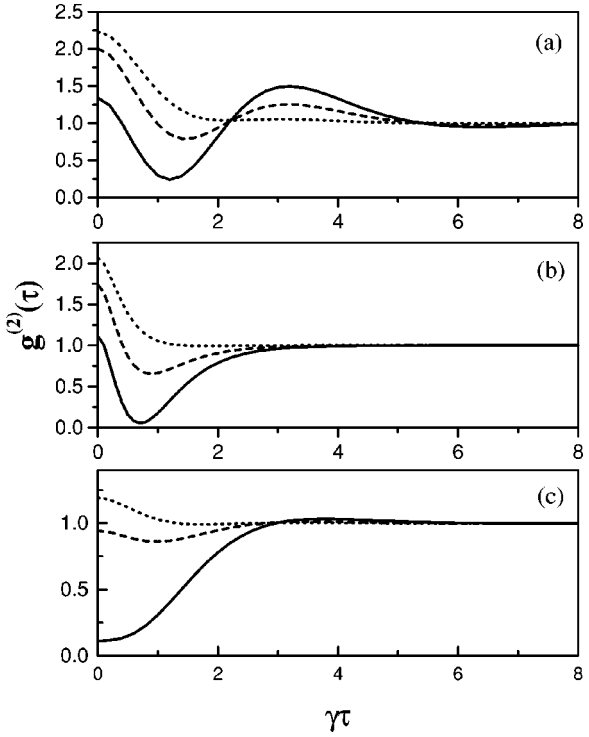

FIG. 6. Photon statistics of the transmitted field with collisional dephasing. The plots are for (a) $g/\gamma=1$, $\kappa/\gamma=0.77$, $E/\gamma=0.1$, $\gamma_{ph}/\gamma=0$ (solid line), 0.05 (dashed line), 0.2 (dotted line); (b) $g/\gamma=2$, $\kappa/\gamma=5$, $E/\gamma=0.1$, $\gamma_{ph}/\gamma=0$ (solid line), 0.05 (dashed line), 0.2 (dotted line); (c) $g/\gamma=1$, $\kappa/\gamma=1.6$, $E/\gamma=0.1$, $\gamma_{ph}/\gamma=0$ (solid line), 0.1 (dashed line), 0.2 (dotted line).

This collapse operator is then applied at a Gaussian distributed series of times with average $1/\gamma_{ph}$ and a full width of $1/\gamma_{ph}$ as this approximates the traversal times of atoms with a Maxwell-Boltzmann velocity distribution. As with any collapse operator, the wave function must be normalized after its application. This model of dephasing differs from collisional dephasing in two important ways. First, it does not enter the deterministic Hamiltonian evolution between collapses at all, whereas the collisional dephasing in the trajectory picture would have a collapse component as well as causing the decay of coherence in the continuous evolution. Second, this dephasing always places the atom into the ground state whereas the collisional dephasing places the atom in the ground or excited state with probabilities determined by the populations. We refer to this second approach as *transit time* dephasing.

Now we turn to our results and a comparison of the two types of dephasing. Because transverse dephasing does not affect the deterministic evolution of the system, we expect that for a given dephasing rate it will be less destructive of the nonclassical photon statistics than collisional dephasing. In Fig. 6 we show the second-order correlation function with collisional dephasing. All three types of nonclassical effect are quite sensitive to this dephasing with $\gamma_{ph}=0.05$ destroying the overshoot [Fig. 6(a)] and undershoot [Fig. 6(b)] while the sub-Poissonian statistics survive until $\gamma_{ph}=0.2$ in Fig. 6(c). Our results for the transit dephasing are shown in Fig. 7. The overshoot in Fig. 7(a) is again extremely sensitive to

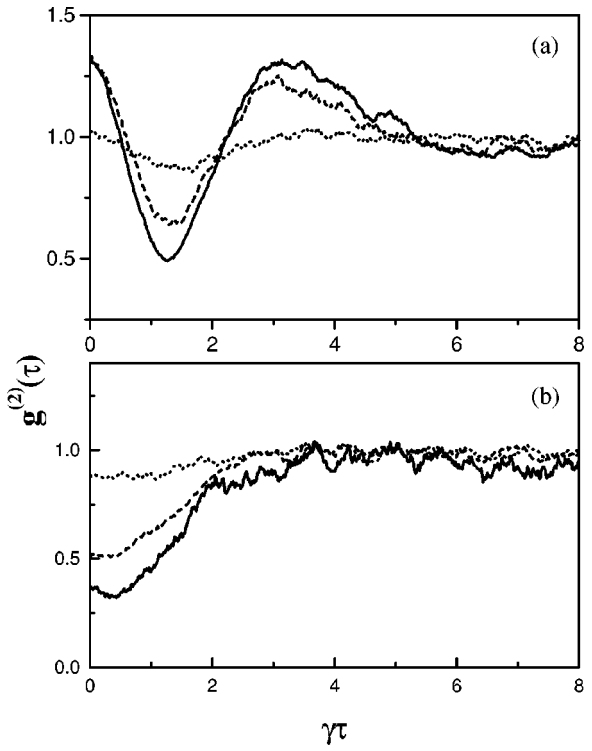

FIG. 7. Photon statistics of the transmitted field with atomic transit dephasing. The plots are for (a) $g/\gamma=1$, $\kappa/\gamma=0.77$, $E/\gamma=0.1$, $\gamma_{ph}/\gamma=0.05$ (solid line), 0.1 (dashed line), 0.5 (dotted line); (b) $g/\gamma=1$, $\kappa/\gamma=1.6$, $E/\gamma=0.1$, $\gamma_{ph}/\gamma=0.05$ (solid line), 0.1 (dashed line), 0.5 (dotted line).

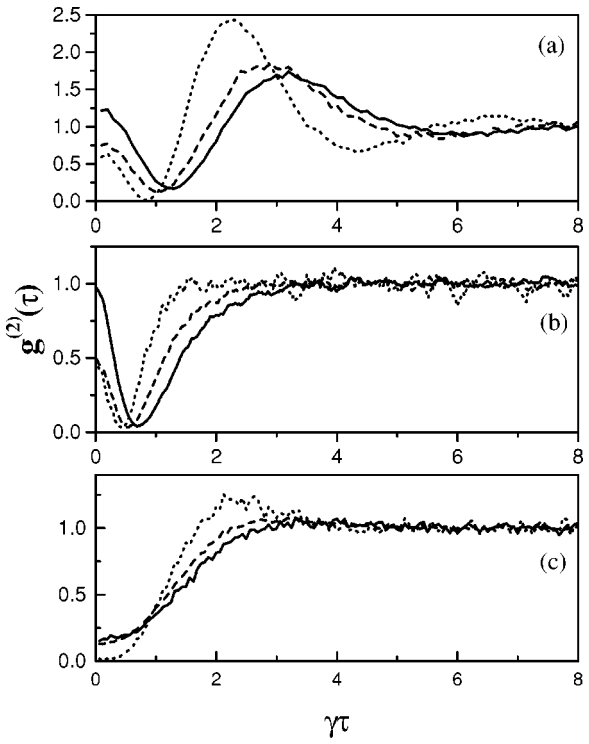

FIG. 8. Photon statistics of the transmitted field with two atoms in the cavity at arbitrary coupling strength. The plots are for (a) $g_1/\gamma=1$, $\kappa/\gamma=0.77$, $E/\gamma=0.1$, $g_2/\gamma=0.1$ (solid line), 0.5 (dashed line), 1 (dotted line); (b) $g_1/\gamma=2$, $\kappa/\gamma=0.77$, $E/\gamma=0.1$, $g_2/\gamma=0.2$ (solid line), 1 (dashed line), 2 (dotted line); (c) $g_1/\gamma=1$, $\kappa/\gamma=1.6$, $E/\gamma=0.1$, $g_2/\gamma=0.1$ (solid line), 0.5 (dashed line), 1 (dotted line).

dephasing with classical statistics for $\gamma_{ph}/\gamma=0.05$ while the sub-Poissonian statistics in Fig. 7(b) are more robust, surviving up to $\gamma_{ph}/\gamma=0.5$. Notice that transit time dephasing is not as destructive to the nonclassical effects as collisional dephasing. This is consistent with experimental results that observe antibunching with transit traversal times on the order of an atomic lifetime [8,9].

V. TWO-ATOM EFFECTS

We now consider the effect of placing two atoms inside the cavity, either both at antinodes of the field, or allowing one of the atoms to be arbitrarily placed so that its coupling is in the range 0 to g_0. Dephasing is not considered in this section. In the experiments conducted on this system it is likely that there is some effect from spectator atoms which are located away from an antinode of the field and so do not contribute to the nonclassical photon statistics. In actuality, as the atoms fly through the cavity, some are strongly coupled and some are not. We refer to the weakly coupled atoms as spectator atoms. If there are enough of these atoms they may simply absorb light and emit it out of the cavity, thus effectively decreasing the quality of the cavity. Are there other effects as well? As a first step toward understanding the effect of spectator atoms, we place one extra atom in the cavity with a coupling that is some fraction of the original atom's coupling. We use a quantum trajectory simulation to calculate photon statistics.

In Fig. 8 we plot $g^{(2)}(\tau)$ while allowing the coupling of the spectator atom (g_2) to vary from $g_0/10$ to g_0. We see that for all three sets of parameters the photon statistics vary continuously from the single-atom result to the two-atom result with no qualitative deviation in the photon statistics. By ''two-atom'' result, we mean the result obtained in [6] for $N=2$ atoms. Recall that the theory in that paper was valid for arbitrary numbers of atoms, but did assume that they all had the same g and were motionless. Also it is noticeable that $N=2$ atoms can have a large amount of antibunching. This is due to the fact that the pair of atoms acts as a collective dipole with $g_{eff}=\sqrt{(N)}g$. The plots in Fig. 8 suggest that the spectator atoms can have an observable effect on the statistics but they do not destroy the nonclassical correlations, at least when close to the ideal condition of having N atoms at antinodes in the cavity. A group of many spectator atoms may be more detrimental to nonclassical correlations.

We now consider the case where both atoms are placed at antinodes of the field. The photon statistics for this system have been solved for arbitrary number of maximally coupled atoms using a set of symmetrized Dicke states to describe the atomic excitation [7]. This would correspond to an experimental setup where it is not possible to tell which atom spontaneously emitted a given photon. The Dicke states are most appropriate when atoms are localized within a wavelength of one another. However, there would be experimental situations where the symmetrized states are not valid states with

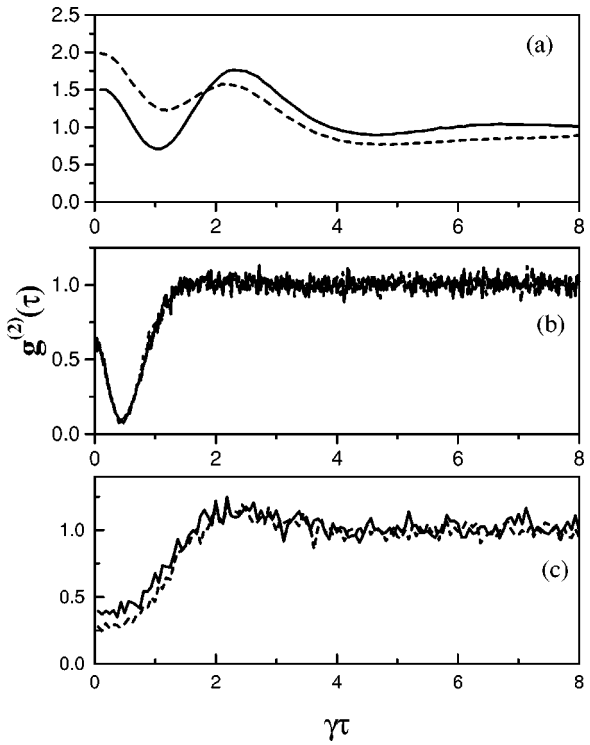

FIG. 9. Photon statistics for the transmitted field with two atoms comparing the symmetrized Dicke spontaneous emission with nonsymmetrized spontaneous emission. The plots are for (a) $g_1/\gamma = g_2/\gamma = 1$, $\kappa/\gamma = 0.77$, $E/\gamma = 0.1$; (b) $g_1/\gamma = g_2/\gamma = 2$, $\kappa/\gamma = 5$, $E/\gamma = 0.1$; (c) $g_1/\gamma = g_2/\gamma = 1$, $\kappa/\gamma = 1.6$, $E/\gamma = 0.1$. The solid line is the nonsymmetrized collapse and the dashed line is the symmetrized collapse.

respect to spontaneous emission. Here, using quantum trajectories, we consider both a symmetrized collapse and an unsymmetrized collapse for spontaneous emission. The operator for the Dicke collapse is

$$\hat{C}_{Dicke} = \frac{1}{\sqrt{2}}(\sigma_-^1 + \sigma_-^2), \tag{21}$$

so that when a spontaneous emission event occurs, both atoms are collapsed symmetrically. For the non-Dicke collapse the atomic operators are used separately so that one atom or the other collapses.

For weak driving field we expect that there will be no difference between these types of collapse because in this limit we detect only photons emitted from steady state. However, for stronger driving fields we begin to detect photons emitted from the collapsed state and the two collapses give different collapsed states ($\sigma_-^1|\psi_{ss}\rangle$ or $\sigma_-^2|\psi_{ss}\rangle$ vs $\hat{C}_{Dicke}|\psi_{ss}\rangle$), and therefore, different photon statistics. Also, if the atoms all have different coupling strengths g_i, the symmetrized Dicke states are not appropriate.

In Fig. 9 $g^{(2)}(\tau)$ is plotted for the two types of collapse for a driving field of $E = 0.5$. Figure 9(a) shows a significant difference as the nonclassical statistics are completely gone for the nonsymmetrized collapse. Figure 9(b) shows no dependence on the type of collapse. Figure 9(c) shows a mild dependence on the type of collapse, with a slightly larger value of $g^{(2)}(0)$ for the nonsymmetrized collapse.

VI. CONCLUSION

We have investigated extensions to previous theoretical work on a driven atoms-cavity system with dissipation. We have calculated the normalized second-order correlation function for the transmitted light including effects of arbitrary driving fields, nonradiative dephasing, and arbitrary coupling strength for multiple atoms. We have found that nonclassical field states are easily destroyed by deviations from the weak field limit and by nonradiative dephasing modeled both as collisional dephasing and as atomic transit dephasing. We have also found that allowing two atoms in the cavity with different atom-field coupling strengths does not have a detrimental effect on the nonclassical field. The experiments that have been done on this system have not really been in the weak field limit. As $E \to 0$ the number of counts also goes to zero, so it is difficult to carry out experiments in this regime, but this work suggests that it is important.

ACKNOWLEDGMENTS

The authors would like to thank Howard J. Carmichael, Luis Orozco, and Greg Foster for many useful conversations.

[1] *Cavity Quantum Electrodynamics*, edited by P. R. Berman Adv. At. Mol. Opt. Phys. Suppl. 2 (1994).
[2] E. T. Jaynes and F. W. Cummings, Proc. IEEE **51**, 89 (1963).
[3] M. Tavis and F. W. Cummings, Phys. Rev. **170**, 379 (1968).
[4] M. Tavis and F. W. Cummings, Phys. Rev. **188**, 692 (1969).
[5] P. R. Rice and H. J. Carmichael, IEEE J. Quantum Electron. **24**, 1351 (1988).
[6] H. J. Carmichael, R. J. Brecha, and P. R. Rice, Opt. Commun. **82**, 73 (1991).
[7] R. J. Brecha, P. R. Rice, and M. Xiao, Phys. Rev. A **59**, 2392 (1999).
[8] G. Rempe *et al.*, Phys. Rev. Lett. **67**, 1727 (1991).
[9] S. L. Mielke, G. T. Foster, and L. A. Orozco, Phys. Rev. Lett. **80**, 3948 (1998).
[10] C. W. Gardiner, *Handbook of Stochastic Methods in Physics, Chemistry, and Natural Sciences* (Springer-Verlag, Berlin, 1983).
[11] H. J. Carmichael, *Statistical Methods in Quantum Optics 1* (Springer-Verlag, Berlin, 1999).
[12] M. Lax, Phys. Rev. **167**, 89 (1967).
[13] H. J. Carmichael, *An Open Systems Approach to Quantum Optics*, Vol. m18 of *Lecture Notes in Physics*, edited by W. Beiglböck (Springer-Verlag, Berlin, 1993).